dynamics

MDPI

Article

Oil Distribution around Ball–Raceway Local Contact Region in Under-Race Lubrication of Ball Bearing

Qingcheng Yu [1], Wenjun Gao [2,*], Ping Gong [1,2], Yuanhao Li [2] and Can Li [2]

[1] AECC Harbin Bearing Co., Ltd., Harbin 150025, China; 13351011369@189.cn (Q.Y.); gongping_0451@163.com (P.G.)
[2] School of Power and Energy, Northwestern Polytechnical University, 127 West Youyi Road, Xi'an 710072, China; liyuanhao0403@163.com (Y.L.); lc13191589130@163.com (C.L.)
* Correspondence: gaowenjun@nwpu.edu.cn

Abstract: The distribution of oil and gas phases around ball–raceway local regions is an important basis and foundation for determining whether a bearing is sufficiently lubricated. To obtain the oil phase distribution law in the inner raceway–ball contact local region (IBCR) and outer raceway–ball contact local region (OBCR) of the ball bearing with under-race lubrication, the numerical simulation method is used. The effects of bearing rotation speed, oil flow rate, oil viscosity, and oil density on these two regions are studied. The results indicate that the oil phase exhibited significant periodic changes in both time and space. Compared with that in the IBCR, the oil phase distribution in the OBCR is more uniform. Increasing the bearing rotation speed and reducing the oil flow rate made the IBCR and OBCR more uniform. Changing the oil viscosity only alters the distribution pattern of the OBCR. The oil density may not affect the fluid flow state or the oil phase distribution in the bearing.

Keywords: numerical simulation; under-race lubrication; ball bearing; local oil distribution; ball–raceway contact

Citation: Yu, Q.; Gao, W.; Gong, P.; Li, Y.; Li, C. Oil Distribution around Ball–Raceway Local Contact Region in Under-Race Lubrication of Ball Bearing. *Dynamics* **2024**, *4*, 731–746. https://doi.org/10.3390/dynamics4030036

Academic Editor: Christos Volos

Received: 23 August 2024
Revised: 11 September 2024
Accepted: 13 September 2024
Published: 19 September 2024

1. Introduction

Rolling bearings are widely used in kinds of rotating mechanical systems because of their low friction coefficient and small starting torque. As supporting rotating components, their working performance has a significant influence on the reliability and stability of the whole mechanical system [1]. In the case of high speed and heavy load, an appropriate amount of oil is needed to lubricate and cool the bearing [2]. For high-speed systems, such as aeroengines and turbines, jet lubrication is usually used [3]. However, as the bearing speed increases, the internal pressure of the bearing increases, making it difficult for the oil to enter the bearing. In under-race lubrication, the oil-supply hole is located on the inner ring. Under the centrifugal force generated by high-speed rotation, oil is supplied into the bearing through radial holes on the inner ring, achieving the lubrication and cooling of the bearing. Therefore, under-race lubrication is usually used at high speeds [4]. For the under-race lubrication of high-speed ball bearings, insufficient oil in the bearing will lead to insufficient lubrication of the bearing, and heat will not be taken away. Excessive oil leads to the viscous friction of the fluid [5]. Under certain mechanisms, the percentage of bearing power loss in the fluid only can reach more than 70% [6]. The viscous friction of the fluid in the bearing is related to the oil phase fraction and oil phase distribution inside the bearing. In addition, the temperature and heat generation of the components in the bearing are also related to the oil phase distribution in the bearing [7], and the operating parameters of the under-race lubrication ball bearing affect the contact-region oil phase distribution and fraction in the bearing [8].

In a ball bearing with under-race lubrication, the interaction between the oil and the bearing components results in complex two-phase flow [9], resulting in different oil phase volume fractions and distributions at different positions of the bearing, which

affects the heat transfer characteristics of the bearing and has an important influence on the thermal performance of the bearing [10]. Jeng et al. [11] established an oil supply condition measurement device for an oil–air lubrication system and a high-speed ball bearing test bench, and the relationship between the oil supply fluctuations and operating parameters of the oil air lubrication system was studied. It was found that smaller injection quantities and smaller injection intervals can improve the stability of the oil supply. The higher the viscosity of the lubricating oil is, the smaller the fluctuation of the oil supply. Flouros [12] studied the two-phase flow in bearings with under-race lubrication. The visualization results of the high-speed camera show that the lubricating oil leaves the bearing through the gap between the cage and the outer ring. Jiang et al. [13] established an oil–air lubrication experimental device for high-speed ball bearings and experimentally researched the performance of ceramic and steel ball bearings under various working conditions. For each speed, there is an appropriate amount of oil to maintain a low temperature increase, and the appropriate amount of oil increases with the increasing speed. Zeng et al. [14] obtained the flow pattern inside a bearing under different working conditions through numerical simulations and experiments. They reported that structural parameters such as the nozzle inclination angle and nozzle diameter strongly influence the distribution of oil–gas two-phase flow. Wu et al. [15] studied stratified gas–oil flow inside a jet-cooled ball bearing. The temperature distribution is affected by the oil volume fraction distribution. The traditional oil injection lubrication mechanism cannot effectively cool the inner ring of a high-speed ball bearing. Yan et al. [16] discussed the oil and gas flow and lubricity of two kinds of ball-bearing lubrication devices and studied and improved their key structural parameters. Finally, the optimal oil supply parameters and operating performance of the two devices were obtained through experimental tests. Bao et al. [17] used the CFD method to simulate the oil–air two-phase flow inside an under-race lubrication ball bearing. As the speed increases, the oil phase volume fraction gradually decreases. Owing to the centrifugal force, the oil is concentrated mainly on the outer ring raceway, which is beneficial for the lubrication and cooling of the outer ring. Peterson et al. [18] established a CFD model of ball bearings and studied the effects of the inner ring speed, the fluid viscosity, the number of rolling elements, and the cage on the internal flow of bearings. Liu et al. [19] established a fluid–solid coupling simulation model based on the CFD method to investigate the lubrication characteristics of oil jet lubrication ball bearings in a gearbox. During the lubrication process, the distribution of oil inside the bearing is not uniform. The average oil volume fraction and oil passing rate decrease with increasing bearing speed and viscosity. Zhang et al. [20] used the CFD method to simulate the transient flow of oil and gas two-phase flow in a jet lubrication roller-sliding bearing. The oil distribution in the bearing is uneven, and it gradually increases from the inner raceway to the outer raceway. Shan et al. [21] proposed a general method for establishing a lubrication analysis model of ball bearings, analyzed the variation in hydrodynamic characteristics such as oil and gas distribution, temperature, and flow rate under different lubrication conditions, and reported that an appropriate gap size can improve the internal flow pattern and hydrodynamic performance of ball bearings.

In summary, the current research on the oil-phase two-phase flow and distribution in bearings has focused mainly on jet lubrication, and the research on the distribution of the oil phase in bearings focuses on the entire bearing cavity, but research on the oil–gas two-phase distribution in under-race lubrication ball bearings is relatively lacking, there is a lack of separate analyses of the oil phase distribution laws in each region of the bearing, and the understanding of the oil–gas two-phase distribution in the ball–raceway local regions of bearings is limited. It is difficult to carry out a more refined design of bearings. One important function of the lubricating oil inside the bearing is the lubrication of the various components inside the bearing, especially the contact regions between the balls and the inner and outer raceways. The distribution of oil phase in the contact region inside the bearing is an important basis and foundation for determining whether the bearing is sufficiently lubricated. Therefore, it is necessary to study the local distribution and

variation in the oil and gas phases in the contact region of the bearing ball under different conditions. Because it is difficult to obtain the oil-gas two-phase flow and distribution in high-speed ball bearings via theory and experiments, this study innovatively separates the ball-race local region of the bearing from the bearing cavity, and the oil and gas two-phase distribution in the ball–raceway local region of the under-race lubrication ball bearing is separately studied through numerical simulation.

2. Model and Method

2.1. Geometric Model

A three-dimensional schematic diagram of the under-race lubrication ball bearing, including the outer ring, inner ring, cage and balls, is shown in Figure 1. There are 6 radial oil supply holes evenly arranged on the inner ring along the circumference, and the lubricating oil flows into the bearing along the oil supply hole through the rotating centrifugal force of the inner ring. After lubrication and cooling in the bearing, the oil flows out of the bearing through the gap between the inner ring and the outer ring of the bearing. The geometric parameters of the ball bearing are shown in Table 1. In actual structure, the contact gap between the balls and the inner/outer raceways is approximately 0.02 mm. To simplify the calculation, the contact gap between the balls and the inner/outer raceways is 0.1 mm, which is larger than the actual structure. This assumption is the standard practice for studying the characteristics of the oil–air two-phase flow inside the bearing [22]. In this study, the bearing load is not considered, and the bearing outlet is at standard atmospheric pressure. The inner ring of the bearing rotates while the outer ring remains stationary. The bearing speed referred to in this paper is the inner ring speed.

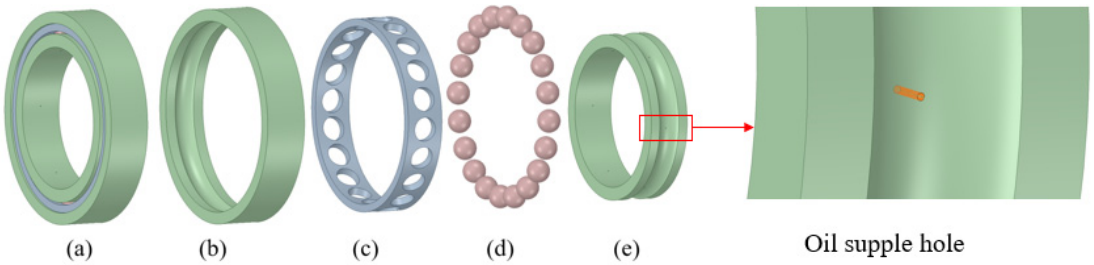

Figure 1. Geometric model of under-race lubrication ball bearing: (**a**) ball bearing, (**b**) outer ring, (**c**) cage, (**d**) balls, (**e**) inner ring.

Table 1. Geometry parameters of ball bearing.

Geometry Parameters	Specification
Inner race diameter/mm	133.35
Outer race diameter/mm	200
Ball diameter/mm	22
Ball number	20
Oil supply hole diameter/mm	1
Inner/outer race curve coefficient	0.52/0.515

2.2. Computational Domain and Mesh

This study focuses only on the inside of the ball bearing, so only the fluid domain of the bearing is retained, and the solid structure of the bearing is discharged. The calculational domain is shown in Figure 2. Because the movement of each part in the bearing is different, the fluid domain is divided into the main flow region, the ball rotation region, the oil supply hole region and the stationary region. 6 oil supply holes are located on the inner ring of the bearing and rotates around the bearing center with the rotation speed of the inner ring, so the rotation speed of the oil supply hole region is the same as that of the inner ring. The

rotation speed of the main flow region inside the bearing is the rotation speed of the cage, and the rotation speed of the cage n_m is:

$$n_m = \frac{n_i}{2}\left(1 - \frac{D\cos\alpha}{d_m}\right) \tag{1}$$

where n_i is the inner ring speed; d_m is the pitch diameter; D is the diameter of the ball; α is the contact angle.

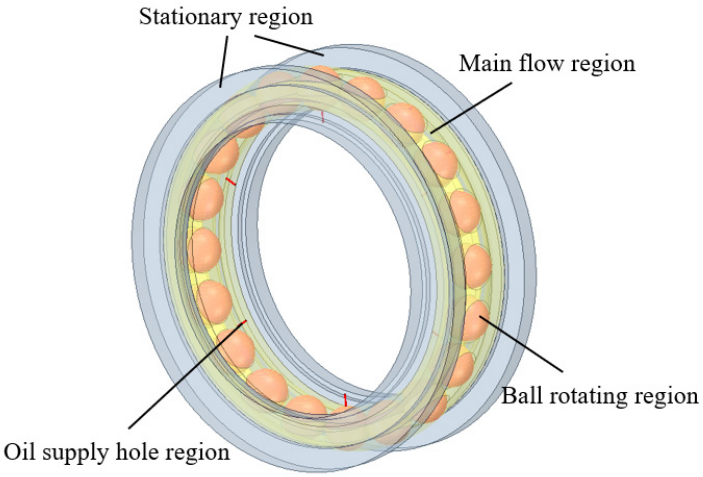

Figure 2. Calculational domain.

The ball rotates around its own axis while rotating around the center of the bearing. The speed of the ball revolution is the same as the speed of the cage, and the self-rotation speed of the balls n_r is [8]:

$$n_r = \frac{d_m n_i}{2D}\left[1 - \left(\frac{D\cos\alpha}{d_m}\right)^2\right] \tag{2}$$

On the one hand, the stationary region on both sides of the bearing provides a reasonable bearing chamber environment for the bearing; on the other hand, it reduces the influence of the reversed flow phenomenon on the calculation results in the numerical calculation.

The software ANSYS Mesh 2020 is employed to discretize the fluid domain, owing to the complex structure of the ball bearing, an unstructured tetrahedral mesh is used to discretize the internal flow field of the bearing, and a structural hexahedral mesh is used to discretize the oil supply hole region. The contact region between the ball and the raceway in the fluid domain and the oil supply hole region are meshed finely to ensure high mesh quality, as shown in Figure 3. To ensure the validity of the numerical results, a grid independence test of the numerical solution is carried out, as shown in Table 2. The results show that increasing the grid density has little effect on the calculation results. Considering the computational cost, the number of cells in the whole computational domain is 3563698, and the number of nodes is 615636.

The 6 oil supply holes located on the inner ring are set as velocity inlets for the calculation model, the two end faces of the stationary region are set as pressure outlets, and the reference pressure is the standard atmospheric pressure. Considering the relative rotational motion between different regions in the bearing, they are related to each other to complete the data transmission. The standard wall function is used near the wall, and the other walls have no-slip boundary conditions.

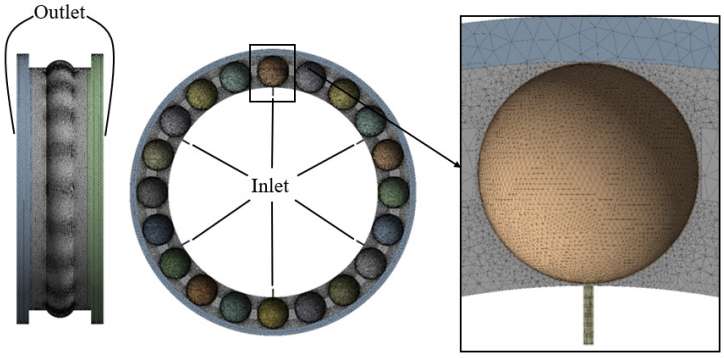

Figure 3. Mesh and boundary conditions.

Table 2. Mesh independence verification.

Number of Grids	Flow Difference between the Inlet and Outlet
2543255	2.86%
3563698	2.45%
4325869	2.33%

2.3. Two-Phase Flow Model

Since the fluid domain in the ball bearing involves oil-gas two-phase flow, the volume of fluid (VOF) method as proposed and implemented in ANSYS Fluent is used in this article. The method allows for the interface between two or more immiscible fluids to be tracked by solving a set of momentum equations. The VOF model uses the volume fraction function to represent the position of the free surface of different fluids and the volume occupied by different fluids, which can better capture the interface of different phases [22]. When φ_{oil} is used to represent the oil phase volume fraction, the following three cases may exist in any given cell:

When $\varphi_{oil} = 0$, the cell is empty of the oil.
When $\varphi_{oil} = 1$, the cell is full of oil.
When $0 < \varphi_{oil} < 1$, the cell contains the interface between the oil and air.

2.4. Turbulence Model

There is a large velocity difference between the parts of the ball bearing at high speed, so a complex turbulent flow will be formed in the bearing [4]. Considering the influence of the high strain rate and large curvature overflow of the bearing and that Renormalization Group k-ε model (RNG k-ε) can improve the accuracy under rotating flow, the RNG k-ε turbulence model is adopted [23]. The modeled transport equations for turbulent kinetic energy (k) and its rate of dissipation (ε) in the RNG k-ε model are given as follows:

$$\frac{\partial}{\partial t}(\rho k) + \frac{\partial}{\partial x_i}(\rho k \mu_i) = \frac{\partial}{\partial x_j}\left[\alpha_k \mu_{eff} \frac{\partial k}{\partial x_j}\right] + G_k - \rho\varepsilon \tag{3}$$

$$\frac{\partial}{\partial t}(\rho \varepsilon) + \frac{\partial}{\partial x_i}(\rho \varepsilon \mu_i) = \frac{\partial}{\partial x_j}\left[\alpha_\varepsilon \mu_{eff} \frac{\partial \varepsilon}{\partial x_j}\right] + C_{1\varepsilon} G_k \frac{\varepsilon}{k} - \rho C_{2\varepsilon} \frac{\varepsilon^2}{k} \tag{4}$$

Among them:

$$\mu_{eff} = \mu + \mu_t \tag{5}$$

$$\mu_t = \rho C_\mu \frac{k^2}{\varepsilon} \tag{6}$$

where μ_i is time-averaged velocity, G_k is the generation of turbulent kinetic energy due to mean velocity gradients, μ_{eff} is effective dynamic viscosity, μ_t is turbulent viscosity, $C_{1\varepsilon}$ and $C_{2\varepsilon}$ are constant terms.

2.5. Numerical Method

The software ANSYS Fluent is used to investigate the Oil distribution around ball–raceway local contact region in under-race lubricating ball bearing. In the numerical calculation, the sliding mesh is used to simulate the motion of each region in the bearing. During initialization, the volume fraction of the gas phase in the whole calculation domain is set to 1, and the volume fraction of the oil phase is set to 0. Air is set as the incompressible main phase, and oil is set as the secondary phase. The type of lubricating oil is Mobil Jet Oil II and the ISO VG Standard is ISO VG 32. The finite volume method is used to discretely solve the governing equation. The central difference scheme is adopted for the diffusion and pressure terms of the momentum equation. The second-order upwind difference was adopted for the convection terms. The pressure was adopted for the PRESTO! (PREssure STaggering Option) format. The semi-implicit method for pressure-linked equations-consistent (SIMPLEC) method is adopted for the coupling solution of pressure and velocity. The convergence of the calculation is judged by the flow difference between the inlet and outlet. When the flow difference between the inlet and outlet is within 3%, the calculation is regarded as convergence, the calculation is stopped, and the calculation results are viewed.

3. Results and Discussion

3.1. Two-Phase Characteristics of Oil and Gas in the Contact Region of a Ball Bearing

Figure 4 shows the oil-gas two-phase distribution in the bearing cavity. The bearing rotation speed is 11,000 rpm, the oil flow rate is 4 L/min, the oil viscosity is 0.0046 Pa·s, and the oil density is 938.6 kg/m^3. After the oil flows out of the oil supply hole, due to the centrifugal force, the oil flows from the inner circulation to the cage pocket and finally flows through the cage pocket to the outer ring region of the bearing. In addition, the oil is unevenly distributed in the bearing. There is more oil near the oil supply hole and less oil away from the oil supply hole. To explore the contact region oil-gas two-phase distribution characteristics in the under-race lubrication ball bearing, the ball bearing is divided into two regions along the radial direction: the inner raceway–ball contact local region (IBCR) and the outer raceway–ball contact local region (OBCR), as shown in Figure 5.

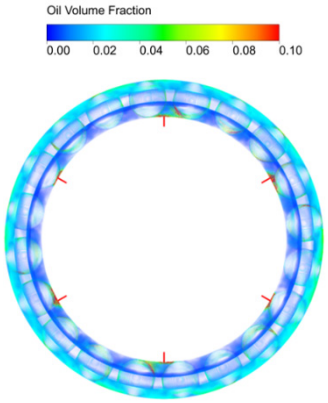

Figure 4. Oil distribution.

Divide the main flow region into 20 parts along the circumference with the ball as the center, and divide each part into IBCR and OBCR. Take the average oil phase volume fraction of IBCR and OBCR, as shown in Figure 6. The oil-phase volume fractions of these two regions along the circumferential direction simultaneously exhibit the largest fluctuation in the IBCR, followed by the OBCR. The oil volume fraction of the OBCR is greater than that of the IBCR; therefore, the lubricating and cooling conditions of the outer raceway–ball contact are better than those of the inner raceway. There are 6 peaks in the circumferential volume fraction of both the IBCR and OBCR samples, which is consistent with the number of oil supply holes. During the operation of the bearing, they are affected

by operating parameters (bearing rotating speed), oil supply parameters (oil flow rate), and lubricating oil properties (oil viscosity and density). Therefore, in the following discussion, we will discuss in detail the impact of these parameters on the oil phase distribution in the local contact area of bearings.

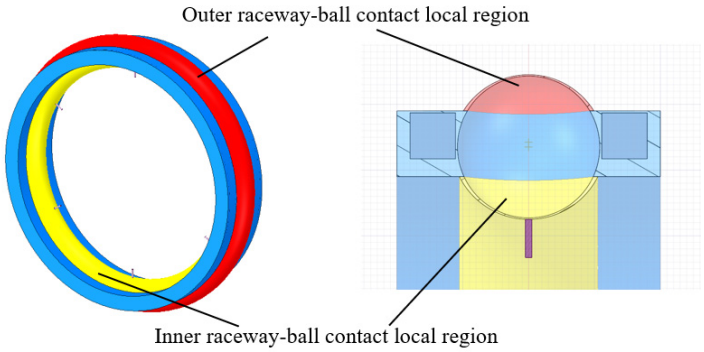

Figure 5. Computational domain division.

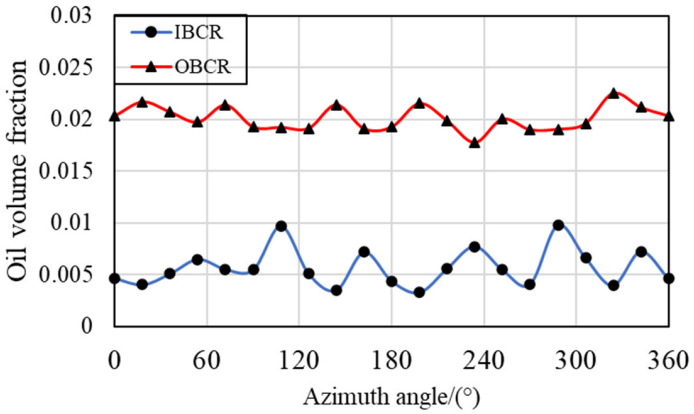

Figure 6. Circumferential oil volume fraction in different regions.

3.2. Effect of the Rotating Speed of the Bearing

As shown in Figure 7, the streamlines around the ball at different bearing rotating speeds are displayed. When the oil enters the bearing through the oil supply hole, a portion of the oil flows out of the bearing through the gap between the inner ring and the cage, whereas another portion of the oil passes through the gap between the balls and the cage to reach the outer ring region of the bearing and finally flows out of the bearing through the gap between the cage and the outer ring. Figure 8 shows the distribution of the oil and gas phases around the ball. After entering the bearing through the oil supply hole, the lubricant oil passes through the gap between the ball and the cage to reach the outer ring region and finally accumulates in the outer ring. As the bearing rotation speed increases, the amount of oil in various regions of the bearing increases.

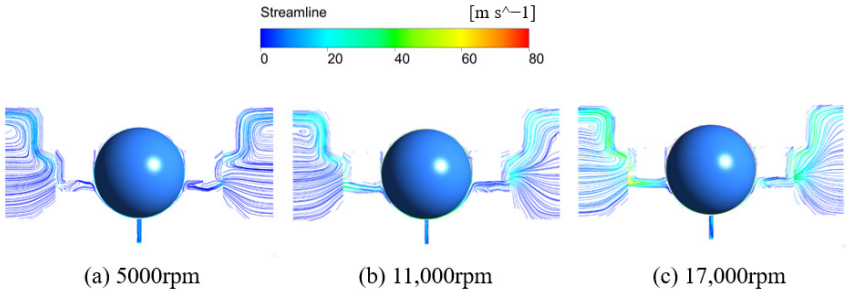

Figure 7. Streamlines at different bearing rotating speeds.

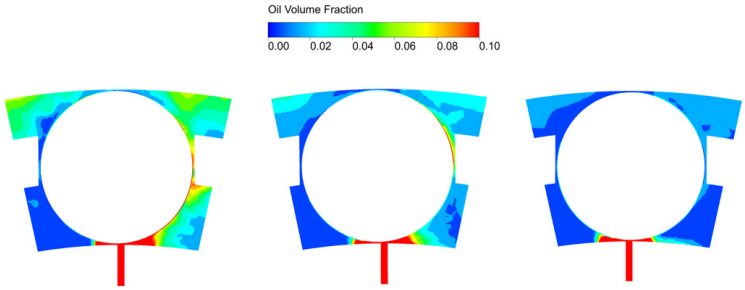

Figure 8. Oil distribution in the contact region at different bearing rotating speeds.

When the bearing rotation speed is 5000 rpm, the volume fraction of the oil phase in the IBCR and OBCR changes over time after one revolution of the bearing, as shown in Figures 9 and 10. The oil clearly has a periodic pattern in the IBCR, and the oil phase increases significantly near the oil supply hole in the OBCR. There is also a periodic pattern in the OBCR, but the fluctuation of the oil phase in the IBCR is greater, and the oil phase distribution in the OBCR is more uniform. Owing to the influence of the centrifugal force of the bearing rotation, the volume fraction of the oil phase in the OBCR is greater than that in the IBCR. As the bearing rotation speed increases, the volume fraction of the oil phase becomes more uniform in both regions, but the volume fraction of the oil phase decreases. Through analysis, the variation in the oil phase volume fraction in the bearing over time can be calculated according to the following formula:

$$N = \frac{n_i - n_m}{n_m} A \tag{7}$$

where N is the number of peak values, n_m is the cage speed, n_i is the inner ring speed, and A is the number of fuel supply holes.

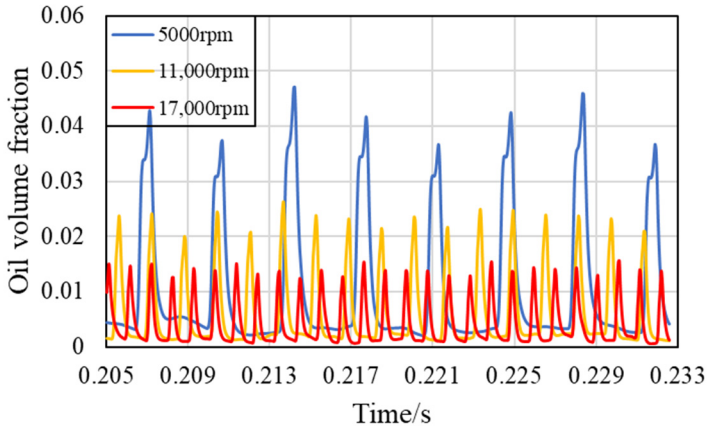

Figure 9. Oil phase volume fraction in the IBCR at different bearing rotating speeds.

When the bearing rotation speed is 5000 rpm, there are 7.8 peaks, whereas the peaks at 11,000 rpm and 17,000 rpm are 2.2 times and 3.4 times greater than those at 5000 rpm, respectively. Therefore, when the bearing rotation speed is 11,000 rpm, there are 17.2 peaks, and when the bearing rotation speed is 17,000 rpm, there are 26.5 peaks, which is consistent with the results shown in Figures 9 and 10.

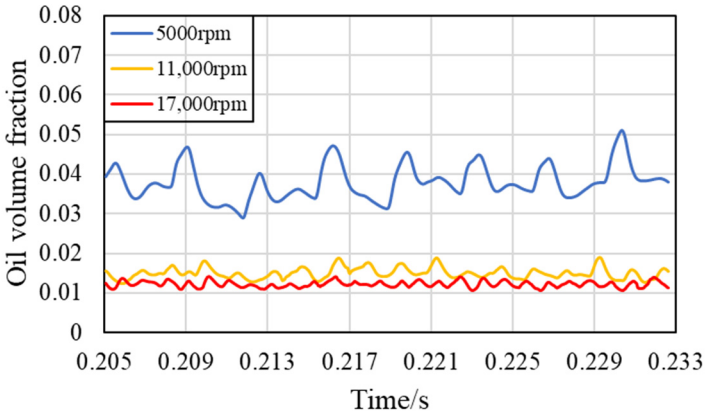

Figure 10. Oil phase volume fraction in the OBCR at different bearing rotating speeds.

Figure 11 shows the volume fraction of the IBCR along the circumferential direction at different bearing rotation speeds. The bearing inner ring region clearly shows a periodic change law, which is related to the number of oil supply holes. There is more oil near the oil supply hole and less oil away from the oil supply hole. Figure 12 shows the volume fraction of the oil phase along the circumferential direction of the OBCR at different bearing rotating speeds. When the bearing rotation speed is 5000 rpm, the periodicity of the outer ring region is more obvious, and when the bearing rotation speed is 17,000 rpm, the periodicity of the outer ring region is not obvious. These two regions in the bearing exhibit a periodic distribution along the circumferential direction at different bearing rotating speeds, and the peak value of the circumferential distribution is consistent with the number of oil supply holes. As the bearing rotation speed increases, the volume fraction of the oil phase in the bearing decreases, and the oil in each region inside the bearing tends to be uniform along the circumferential direction. At high speeds, the amount of lubricating oil inside the bearing is relatively small, which may lead to insufficient lubrication and cooling. Therefore, increasing the lubricating oil flow rate should be considered at high speeds. Through analysis, it can be concluded that the spatial distribution pattern is consistent with the temporal variation pattern. In the following analysis, only the spatial distribution pattern is studied.

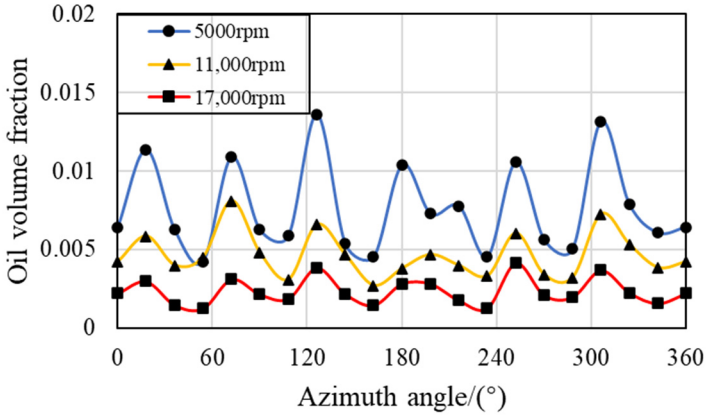

Figure 11. Circumferential oil phase volume fraction in the IBCR at different rotation speeds.

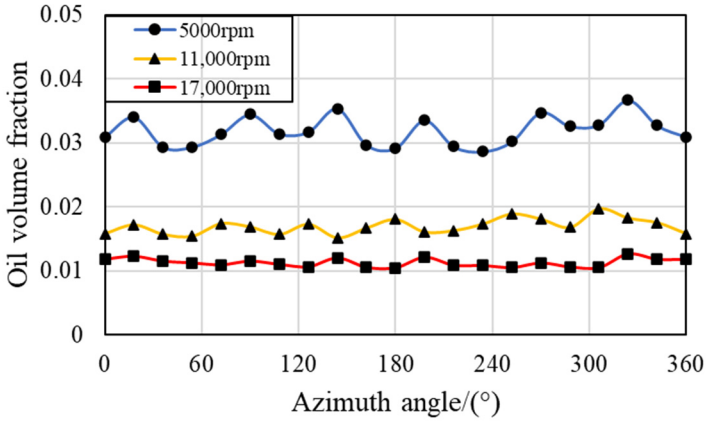

Figure 12. Circumferential oil phase volume fraction in the OBCR at different rotation speeds.

3.3. Effect of the Oil Flow Rate

Figure 13 shows the streamlines at different flow rates. When the oil flow rate changes, the bearing rotation speed remains unchanged, and the relative motion of various components inside the bearing also remains unchanged. Therefore, the fluid velocity inside the bearing remains essentially unchanged. As shown in Figure 14, when the oil flow rate increases to 6 L/min, the increase in oil volume in the bearing leads to an increase in the oil phase volume fraction in various regions.

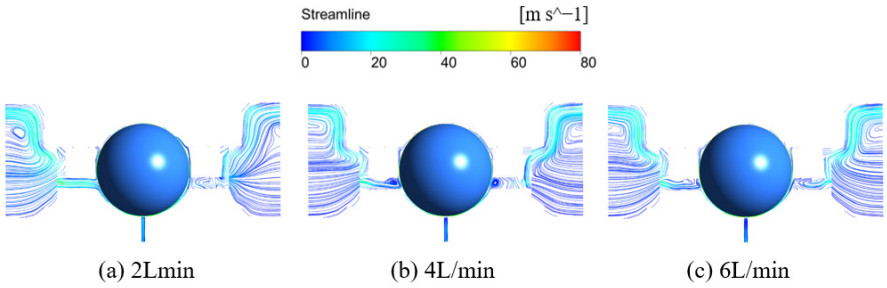

Figure 13. Streamlines at different oil flow rates.

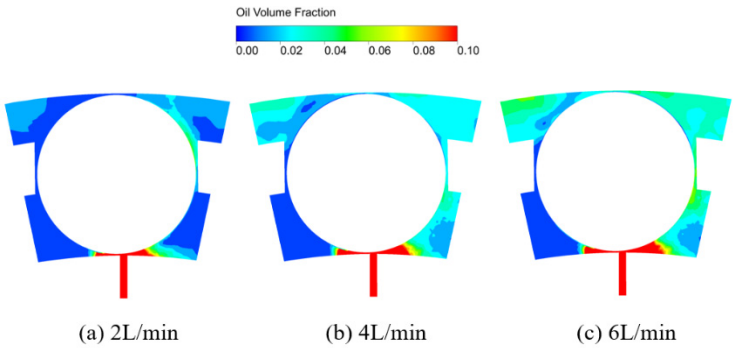

Figure 14. Oil distribution in the contact region at different oil flow rates.

Figures 15 and 16 show the volume fraction of the oil phase along the circumferential direction of the IBCR and OBCR at different bearing rotating speeds. The oil phase distribution in the two regions has periodicity. After entering the bearing through the oil supply hole, the oil flows toward the outer ring region, causing the oil to concentrate mainly in the OBCR. The amount of oil in the IBCR is low, and the oil supply hole is located on the inner ring. Therefore, compared with OBCR, the periodicity of IBCR is more obvious. When the oil flow rate is 2 L/min, the oil distribution in the OBCR is still very even. When the oil flow rate increased to 6 L/min, significant fluctuations appeared. Accordingly, as the oil flow

rate increases, the circumferential distribution in various regions of the bearing becomes increasingly uneven. When the oil flow rate is low, it can lead to insufficient lubrication in the bearing and difficulty in removing heat. When the oil flow rate is high, it can cause severe fluid viscous friction in the bearing and generate a large amount of heat. Therefore, the oil flow rate should be maintained within an appropriate range.

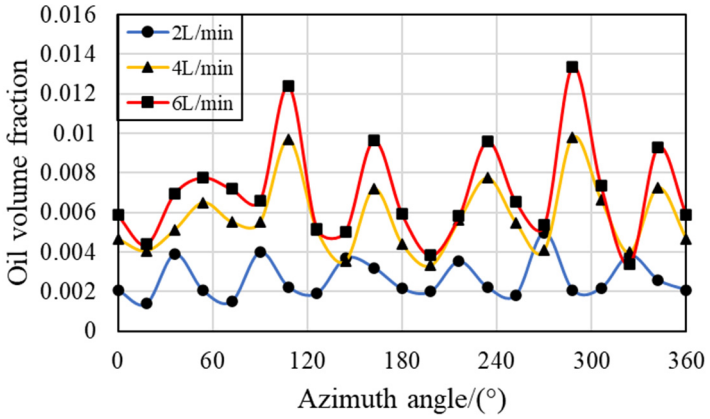

Figure 15. Circumferential oil phase volume fraction in the IBCR at different oil flow rates.

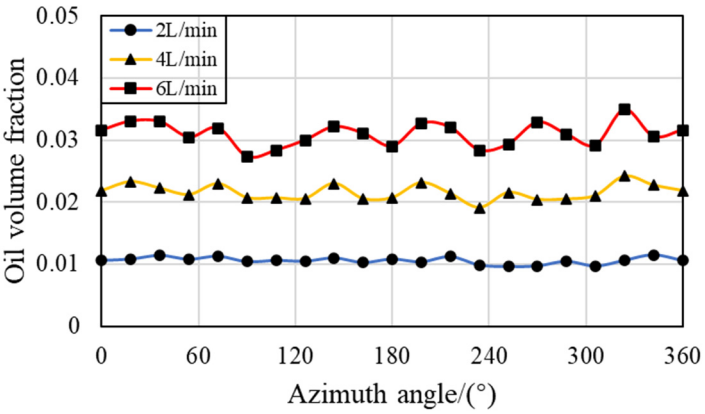

Figure 16. Circumferential oil phase volume fraction in the OBCR at different oil flow rates.

3.4. Effects of Oil Viscosity

During the movement of the bearing, the physical properties of the fluid inside the bearing, such as viscosity, change with temperature. Figure 17 shows the streamline diagram at different oil viscosities. As the oil viscosity changes, the velocity of the fluid inside the bearing remains essentially unchanged. Figure 18 shows the oil-gas two-phase distribution in the contact region of the bearing under different oil viscosities. As the viscosity of the lubricating oil increases, the amount of oil inside the bearing increases and is concentrated in the outer ring region, which is consistent with the changes in the rotating speed and flow rate of the bearing.

Figure 19 shows the volume fraction of the oil phase along the circumferential direction of the IBCR at different oil viscosities. When the oil viscosity is changed, the volume fraction of the oil phase in the IBCR of the bearing remains essentially unchanged. Compared with that in the IBCR, the volume fraction of the oil phase in the OBCR increases with increasing oil viscosity, as shown in Figure 20. Therefore, increasing the viscosity of the oil mainly affects the volume fraction of the oil phase in OBCR. By changing the oil viscosity, the periodicity of these two regions remains unchanged. An increase in oil viscosity will lead to an increase in the volume fraction of the oil phase inside the bearing, and also increase the viscous friction inside the bearing. Therefore, the oil viscosity should be kept reasonable.

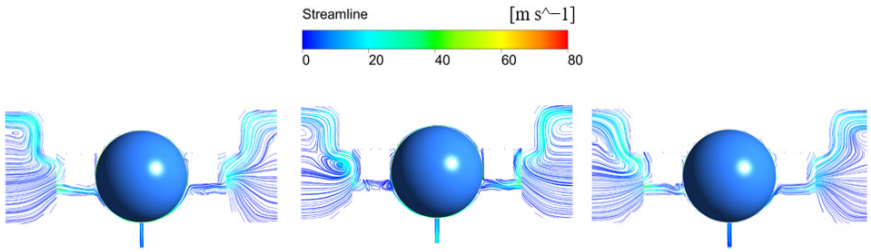

Figure 17. Streamlines at different oil viscosities.

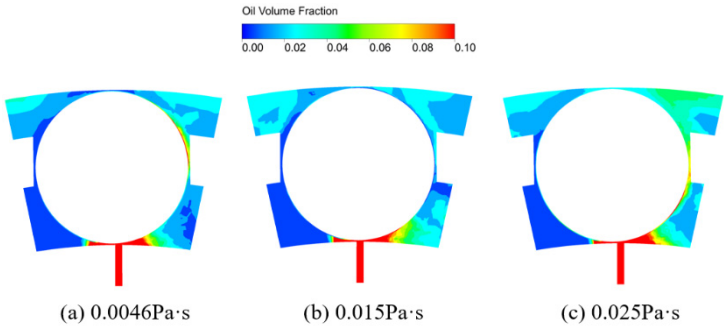

Figure 18. Oil distribution in the contact region at different oil viscosities.

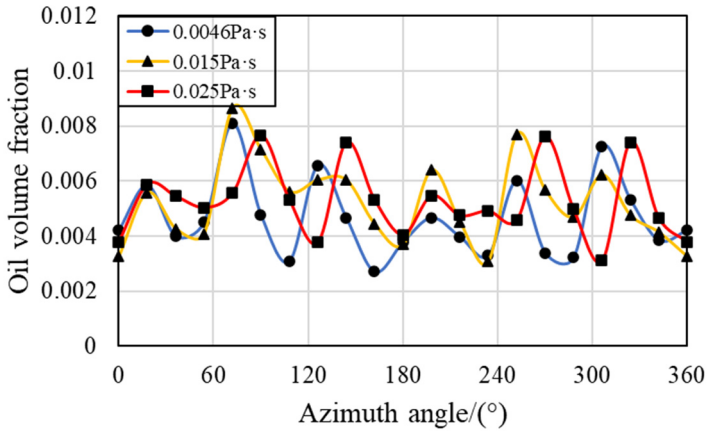

Figure 19. Circumferential oil phase volume fraction in the IBCR at different oil viscosities.

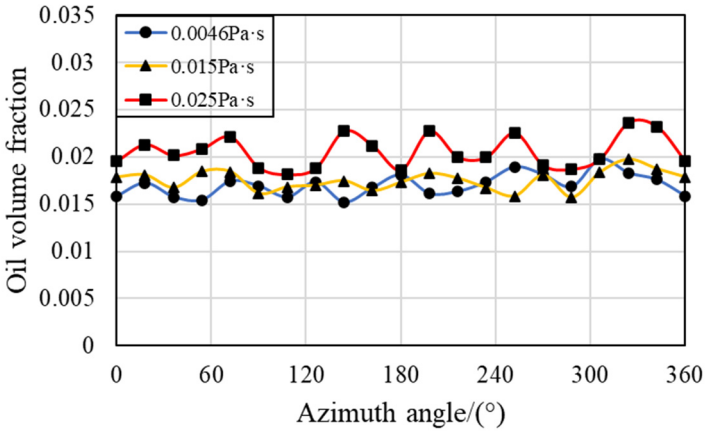

Figure 20. Circumferential oil phase volume fraction in the OBCR at different oil viscosities.

3.5. Effect of Oil Density

During the movement of the bearing, the fluid density also changes. When the oil density is changed, the fluid velocity and flow state inside the bearing remain basically unchanged, as shown in Figure 21. Figure 22 shows that the two-phase distribution of oil in the bearing remains unchanged. The variation law and periodicity of the oil-gas two-phases in the IBCR and OBCR of the bearing also remain unchanged, as shown in Figures 23 and 24. When analyzing the distribution of oil phase in bearings, the other three variables (bearing rotating speed, oil flow rate and oil viscosity) can be considered as key factors.

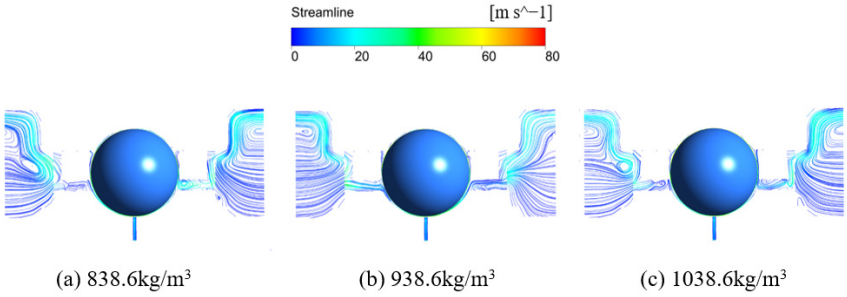

Figure 21. Streamlines at different oil densities.

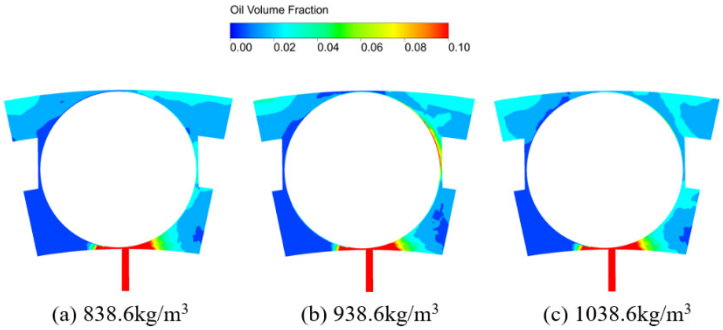

Figure 22. Oil distribution in the contact region at different oil densities.

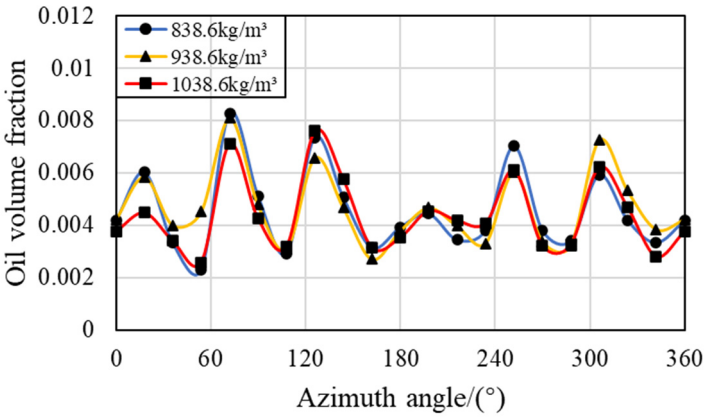

Figure 23. Circumferential oil phase volume fraction in the IBCR at different oil densities.

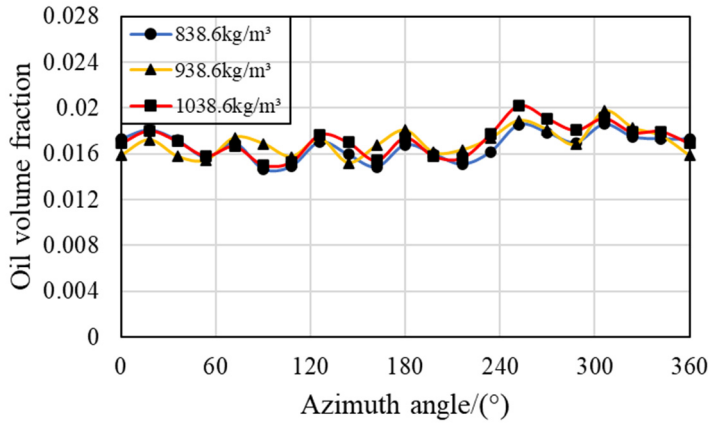

Figure 24. Circumferential oil phase volume fraction in the OBCR at different oil densities.

4. Conclusions

In this work, a model of under-race lubrication ball bearing is established, and the oil-gas two-phase distribution in the ball–raceway contact local region of the bearing is studied via a numerical simulation method. The motion state of the fluid in the inner raceway–ball contact local region (IBCR) and the outer raceway–ball contact local region (OBCR), as well as the distribution of the oil and gas phases with changes in the rotating speed, oil flow rate, oil viscosity and oil density of the bearing, are studied. The salient findings are summarized as follows:

(1) There is a clear periodic variation pattern in the IBCR and OBCR of the bearing over time and space. In terms of time, periodicity is related to the number of oil supply holes, the speed of the cage, and the speed of the inner ring. The period in space is related only to the number of oil supple holes.

(2) The oil distribution inside the bearing is uneven, with more oil near the oil supply hole in the circumferential direction, and it is mainly concentrated in the outer ring region in the radial direction because of the centrifugal force caused by the rotation of the bearing. Compared with that in the IBCR, the oil phase distribution in the OBCR is more uniform.

(3) Increasing the bearing rotation speed reduces the oil volume fraction in the IBCR and OBCR, resulting in a more uniform distribution of the oil phase. Increasing the oil flow rate results in an increase in the oil volume fraction of the IBCR and OBCR and an increase in fluctuations in the oil phase distribution. Increasing the oil viscosity only increases the oil volume fraction of the OBCR and causes an increase in fluctuations in the OBCR. The oil density does not affect the volume fraction or uniformity of the oil phase.

(4) Compared with the outer raceway–ball contact region, it is more difficult to keep lubricating oil in the inner raceway–ball contact region. If the oil supply condition becomes worse or the bearing rotates faster, it is easier for the inner raceway to experience lubrication failure and frictional wear.

This study has to some extent enabled us to understand the distribution law of oil and gas two-phase in the contact region of the under-race lubrication ball bearing. The viscous friction and heat transfer inside the bearing should be added in the next step, which is our ongoing study.

Author Contributions: Conceptualization, Q.Y. and W.G.; methodology, P.G.; software, Y.L. and C.L.; validation, W.G. and P.G.; writing—original draft preparation, W.G. and P.G.; visualization, Q.Y. and Y.L.; funding acquisition, W.G. All authors have read and agreed to the published version of the manuscript.

Funding: This research was funded by the Key Research and Development Program of Shaanxi (Grant number: 2024GX-YB-XM-014), Science Center for Gas Turbine Project (Grant number: P2022-B-III-003-001), and the National Science and Technology Major Project of China (Grant number: J2019-III-0023-0067).

Data Availability Statement: The original contributions presented in the study are included in the article, further inquiries can be directed to the corresponding author.

Conflicts of Interest: Author Qingcheng Yu was employed by the company AECC Harbin Bearing Co., Ltd. The remaining authors declare that the research was conducted in the absence of any commercial or financial relationships that could be construed as a potential conflict of interest.

References

1. Gao, W.; Nelias, D.; Li, K.; Liu, Z.; Lyu, Y. A multiphase computational study of oil distribution inside roller bearings with under-race lubrication. *Tribol. Int.* **2019**, *140*, 105862. [CrossRef]
2. Gloeckner, P.; Dullenkopf, K.; Flouros, M. Direct outer ring cooling of a high speed jet engine mainshaft ball bearing: Experimental investigation results. *J. Eng. Gas. Turbines Power* **2011**, *133*, 062503. [CrossRef]
3. Pinel, S.I.; Signer, H.R.; Zaretsky, E.V. Comparison between oil-mist and oil-jet lubrication of high-speed, small-bore, angular-contact ball bearings. *Tribol. Trans.* **2001**, *44*, 327–338. [CrossRef]
4. Jiang, L.; Lyu, Y.; Gao, W.; Zhu, P.; Liu, Z. Numerical Investigation of the Oil–Air Distribution Inside Ball Bearings with Under-Race Lubrication. *Proc. Inst. Mech. Eng. Part J J. Eng. Tribol.* **2022**, *236*, 499–513. [CrossRef]
5. Gao, W.; Lyu, Y.; Liu, Z.; Nelias, D. Validation and application of a numerical approach for the estimation of drag and churning losses in high speed roller bearings. *Appl. Therm. Eng.* **2019**, *153*, 390–397. [CrossRef]
6. Zhao, Y.; Zi, Y.; Chen, Z.; Zhang, M.; Zhu, Y.; Yin, J. Power loss investigation of ball bearings considering rolling-sliding contacts. *Int. J. Mech. Sci.* **2023**, *250*, 108318. [CrossRef]
7. Wu, W.; Hu, C.; Hu, J.; Yuan, S.; Zhang, R. Jet cooling characteristics for ball bearings using the VOF multiphase model. *Int. J. Therm. Sci.* **2017**, *116*, 150–158. [CrossRef]
8. Gao, W.; Li, C.; Li, Y.; Liu, Z.; Lyu, Y. Oil–Air Two-Phase Flow Distribution Characteristics inside Cylindrical Roller Bearing with Under-Race Lubrication. *Lubricants* **2024**, *12*, 133. [CrossRef]
9. Marchesse, Y.; Changenet, C.; Ville, F. Numerical investigations on drag coefficient of balls in rolling element bearing. *Tribol. Trans.* **2014**, *57*, 778–785. [CrossRef]
10. Yan, K.; Wang, Y.; Zhu, Y.; Hong, J.; Zhai, Q. Investigation on heat dissipation characteristic of ball bearing cage and inside cavity at ultra high rotation speed. *Tribol. Int.* **2016**, *93*, 470–481. [CrossRef]
11. Jeng, Y.-R.; Gao, C.-C. Investigation of the ball-bearing temperature rise under an oil-air lubrication system. *Proc. Inst. Mech. Eng. Part J J. Eng. Tribol.* **2001**, *215*, 139–148. [CrossRef]
12. Flouros, M. Reduction of Power Losses in Bearing Chambers Using Porous Screens Surrounding a Ball Bearing. *J. Eng. Gas. Turbines Power* **2005**, *128*, 178–182. [CrossRef]
13. Jiang, S.; Mao, H. Investigation of the high speed rolling bearing temperature rise with oil-air lubrication. *J. Tribol.* **2011**, *133*, 021101. [CrossRef]
14. Zeng, Q.; Zhang, J.; Hong, J.; Liu, C. A comparative study on simulation and experiment of oil-air lubrication unit for high speed bearing. *Ind. Lubr. Tribol.* **2016**, *68*, 325–335. [CrossRef]
15. Wu, W.; Hu, J.B.; Yuan, S.H. Numerical and experimental investigation of the stratified air-oil flow inside ball bearings. *Int. J. Heat Mass Transf.* **2016**, *103*, 619–626. [CrossRef]
16. Yan, K.; Zhang, J.H.; Hong, J.; Wang, Y.T.; Zhu, Y.S. Structural optimization of lubrication device for high speed angular contact ball bearing based on internal fluid flow analysis. *Int. J. Heat Mass Transf.* **2016**, *95*, 540–550. [CrossRef]
17. Bao, H.; Hou, X.; Lu, F. Analysis of oil-air two-phase flow characteristics inside a ball bearing with under-race lubrication. *Processes* **2020**, *8*, 1223. [CrossRef]
18. Peterson, W.; Russell, T.; Sadeghi, F.; Berhan, M.T.; Stacke, L.-E.; Ståhl, J. A CFD investigation of lubricant flow in deep groove ball bearings. *Tribol. Int.* **2021**, *154*, 106735. [CrossRef]
19. Liu, J.; Ni, H.; Xu, Z.; Pan, G. A simulation analysis for lubricating characteristics of an oil-jet ball bearing. *Simul. Model. Pract. Theory* **2021**, *113*, 102371. [CrossRef]
20. Zhang, J.J.; Lu, L.M.; Zheng, Z.Y.; Gan, L.; Lv, Z.Y. Visual comparative analysis for the oil-air two-phase flow of an oil-jet lubricated roller-sliding bearing. *J. Appl. Fluid Mech.* **2022**, *16*, 179–191.
21. Shan, W.; Chen, Y.; Huang, J.; Wang, X.; Han, Z.; Wu, K. A multiphase flow study for lubrication characteristics on the internal flow pattern of ball bearing. *Results Eng.* **2023**, *20*, 101429. [CrossRef]

22. Hirt, C.W.; Nichols, B.D. Volume of fluid (VOF) method for the dynamics of free boundaries. *J. Comput. Phys.* **1981**, *39*, 201–225. [CrossRef]
23. Xiao, J.; Zhu, E.; Wang, G. Numerical simulation of emergency shutdown process of ring gate in hydraulic turbine runaway. *J. Fluids Eng.* **2012**, *134*, 124501. [CrossRef]